Reaction Kinetics, Mechanisms and Catalysis (2019) 126:477–495
https://doi.org/10.1007/s11144-018-1470-5

The effect of Ce, Zn and Co on Pt-based catalysts in propane dehydrogenation

Maryam Naseri[1] · Farnaz Tahriri Zangeneh[2] · Abbas Taeb[1]

Received: 7 September 2018 / Accepted: 9 September 2018 / Published online: 20 September 2018

Abstract

The effect of the addition of different promoters, such as, Ce, Zn and Co (0.3, 0.5 and 0.7 wt%) to the trimetallic Pt–Sn–K/Al_2O_3 catalyst in order to enhance performance of propane dehydrogenation was investigated and characterized with several analytic techniques, including, TPR, XRF, UV analysis, SEM and TGA–DTA. The catalysts were prepared by sequential impregnation of γ-Al_2O_3 technique. It was found that suitable addition of Zn (0.7 wt%), Ce (0.5 wt%) and Co (0.3 wt%) to the Pt–Sn–K/γ-Al_2O_3 catalyst can improve the catalytic performance more than the commercial Pt–Sn/γ-Al_2O_3 catalyst. The best results on Sn reduction was obtained by adding Zn (0.7 wt%) and Co (0.3 wt%) to the trimetallic Pt–Sn–K/Al_2O_3 catalyst. Ce (0.5 wt%) due to its ability on Pt reduction peak temperature was able to reveal better result. The performance of Pt–Sn–K–$Ce_{0.5}$–$Zn_{0.7}$/γ-Al_2O_3 and Pt–Sn–K–$Co_{0.3}$–$Zn_{0.7}$/γ-Al_2O_3 catalysts were improved by a suitable amount of Ce, Zn and Co Pt–Sn–K–$Co_{0.3}$–$Zn_{0.7}$/γ-Al_2O_3 showed better performance in terms of conversion and propylene selectivity. The synergic effect of Co and Zn can enlarge the Pt reduction peak areas than Pt–Sn–K–$Co_{0.3}$/γ-Al_2O_3 and Pt–Sn–K–$Zn_{0.7}$/γ-Al_2O_3, so can suppress the coke formation and improve the catalyst performance.

Keywords Dehydrogenation · Pt–Sn Catalyst · Promoter · Propane

Electronic supplementary material The online version of this article (https://doi.org/10.1007/s11144-018-1470-5) contains supplementary material, which is available to authorized users.

✉ Farnaz Tahriri Zangeneh
tahriri_zangeneh@yahoo.com

[1] Department of Chemistry Engineering, Iran University of Science and Technology, Tehran, Tehran 16846-13114, Iran

[2] Catalyst Research Group, Petrochemical Research and Technology Company, National Petrochemical Company, Tehran, Tehran 14358-84711, Iran

Introduction

The global demand for propylene as the feedstock for a variety of polymers and intermediates in the chemical industry has been expanded [1, 2]. Currently, the main source for propylene is from by-production of gasoline by both thermal and catalytic cracking [3]. Propane dehydrogenation not only has a great potential in the use of light paraffins for propylene boosters, but also it can decrease the gap between the supply and demand for propylene [4].

Platinum-based mono- and bimetallic (Pt–Sn) catalysts supported on γ-Al_2O_3 have been widely used in hydrocarbon dehydrogenation, but bimetallic platinum-tin catalysts show relatively high reaction conversion and selectivity [4–6]. The improvement of the stability and selectivity for paraffin dehydrogenation to olefins is increased, while cracking process, isomerization reactions, and the coke formation process are suppressed [1, 3, 7]. Significant progress in the PtSn catalyst has been reported in a large number of papers [5, 8, 9]. Generally, the catalytic properties of bimetallic Pt–Sn catalysts strongly depend on interaction between Pt and Sn, as well as the state of Sn [5, 6, 10].

The roles of Sn is mainly an electronic and geometric effects modifying the Pt. The geometric effect of tin is reducing the size of platinum ensembles, hydrogenolysis and coking reactions requiring a large part of ensembles [11]. The electronic modification of Sn on Pt consists of the positive charge transfer from Sn^{n+} species and different electronic structures of PtSn alloys [9, 12, 13].

Tasbihi et al. [7] found that adding K and Li to PtSn/γ-Al_2O_3 lead to better catalytic performance. They also compared it with the PtSn/γ-Al_2O_3 catalyst. Nagaraja [14] found that the addition of a small amount of K on the bimetallic PtSn/γ-Al_2O_3 catalyst improved the n-$C_4^=$ yield. Potassium blocks the acid sites of Pt catalyst, improving the selectivity. Siri [11] reported that the addition of K in the dehydrogenation reaction improved the stability level of the catalyst. However, the dehydrogenation performance of PtSn catalysts is still not satisfactory, especially with regard to the stability of the catalysts. Therefore, it is necessary to improve the catalytic stability of supported PtSn catalysts during light paraffin conversion.

Lanthanum and cerium are rare earth elements showing unique effects which are related to the strong metal-rare earth oxide interaction and the thermal stabilization of the alumina support [3, 15]. Navarro [16] and others studied the effect of Ce and La on the PtNi-catalyst that supported on Al_2O_3 for acetone steam reforming. The main roles of CeO_2 were promoting the thermal stability of γ-Al_2O_3, which was attributed to the $CeAlO_3$ formation [1, 3–20].

Zn and Co, as transition metals, can increase the electron density of Pt, suppressing the coke formation. The effect of Zn on Pt can be related to the strong interactions between zinc and platinum due to the formation of PtZn alloy and the change in the electronic properties of Pt atoms (e.g., the formation of $Pt^{\delta-}$–$Zn^{\delta+}$ entities) [13]. Zhang et al. [10] investigated the effect of zinc addition on the catalytic properties of the Pt–Sn–K/γ-Al_2O_3 catalyst for isobutane dehydrogenation. They reported that the suitable addition of Zn to Pt–Sn–K/γ-Al_2O_3 could decrease

the carbon depositions, resulting in the geometric effect and stabilizing the oxidation state of Sn species.

Guczi et al. [21] investigated the structure of Pt–Co/Al_2O_3 and Pt–Co/NaY bimetallic catalysts in Co hydrogenation. On the other hand, Dietrich et al. [22] investigated the effect of Co and Mo as promoters on Pt-based aqueous phase reforming catalysts. However, comparatively few papers have reported the effects of cobalt on alumina supported platinum catalysts in propane dehydrogenation.

The mechanisms of dehydrogenation of alkane have been studied in several investigations. Biloen et al. [23] studied the catalytic dehydrogenation of propane to propylene over platinum and platinum–gold alloys. They proposed that dissociative chemisorption of propane on a single platinum atom to which two adsorption sites are associated, one of which carries a hydrogen atom. The subsequent conversion of the propyl radical into π-bonded propylene via β-hydrogen elimination was the rate determining step. The last step, desorption of r-bonded propylene had a comparatively low activation energy. Also Slatter [24] in the case of side reactions stated, catalytic cracking requires a catalyst with Brønsted and/or Lewis acidity and proceeds via the formation of a carbocation intermediate, and it leads the formation of an alkenes and an alkane. Isomerization is the rearrangement of atoms within a molecule. He acknowledged that the balance between dehydrogenation and these side reactions is very complex. Although catalysts have effects on the reaction mechanism, but in this study we have not investigated the reaction mechanism. We have tried to eliminate side reaction by using proper promoters.

In the present study, Pt–Sn–K–M/γ-Al_2O_3 (M: Zn, Ce and Co) catalysts with different contents of zinc, cerium and cobalt were prepared for the dehydrogenation of propane. The catalysts were analyzed by several techniques including TPR, XRF, UV, SEM, and TG–DTA.

Experimental

Catalyst preparation

A series of Pt–Sn–K–M/γ-Al_2O_3 catalysts with different M metals (M = Zn, Ce and Co) as the promoter were prepared by a sequential impregnation method. A commercial γ-Al_2O_3 (S_{BET} = 215 m^2/g) previously calcined in air at 550 °C for 2 h was used as a support. The M/γ-Al_2O_3 catalyst was prepared by impregnating the metal from an excess aqueous solution of the fourth metal (M = Zn, Ce and Co) precursor (metal nitrate hexahydrate). After impregnation, it was dried at 120 °C overnight and calcined at 550 °C, with a rate of 5 °C/min in air for 2 h. Then Sn was impregnated from Sn precursor (Tin(II) chloride dihydrate) on the prepared (M)/γ-Al_2O_3. The Sn-M/γ-Al_2O_3 catalyst was prepared using hydrochloric acid; this was followed by drying at 120 °C overnight and calcination at 550 °C in air for 2 h. For the preparation of the Pt–Sn–M/γ-Al_2O_3 catalyst, the Pt precursor (hexachloroplatinic acid hexahydrate) was impregnated in a fixed-bed quartz reactor (ID = 2.0 cm, L = 23 cm). The impregnating solution (40 ml) was passed and totally recycled to the support-bed (10 g) by two peristaltic pumps. For the preparation of the Pt–

Sn–K–M/γ-Al_2O_3 catalyst, K precursor (potassium nitrate trihydrate) was dry impregnated on the prepared Pt–Sn–M/γ-Al_2O_3. The contents of Pt, Sn, K, and the fourth metal in the Pt–Sn–K–M/γ-Al_2O_3 catalysts were fixed at 0.5 wt%, 0.71 wt%, 0.65 wt%, and 0.3–0.5–0.7 wt%. For reference, the commercial Pt–Sn/γ-Al_2O_3 catalyst named PD-IND, as supplied by a European company [25], was used as the reference for the performance.

Characterization methods

XRF

X-ray fluorescence (XRF) measurements on a Philips PW2404 XRF analyzer could determine the Platinum, tin, and chlorine content of the samples.

TPR

Temperature-programmed reduction experiments were carried out on an BELCAT-Aanalyzer consisting of a programmable temperature furnace. Samples (0.2 g) were filled in the quartz reactor. The furnace was heated to 850 °C at a rate of 10 °C/min in 7.52% H_2/Ar stream (50 ml/min). The effects of promoters on the reduction properties of catalysts were studied by TPR.

SEM

In order to determine the uniformity of the layer deposited by impregnation on catalyst, characterization was done by scanning electronic microscope (SEM), with a VEGA\TESCAN analyzer. To ensure the sample conductivity, they were coated with a thin layer of gold. SEM had an EDAX detector that could measure the wavelength and Pt adsorption as a small X-ray fluorescence.

TG-DTG

The carbon content of the used catalysts was measured by a thermogravimetry/differential thermal analysis (TG-DTG) instrument (Terkimelmer instrument diamond). The sample was heated to 1100 °C at a heating rate of 10 °C/min and in an air flow of 50 ml/min.

UV–vis spectroscopy

The platinum concentration within the solution container was measured by Metrohm 744 UV–Vis spectrometer after Pt impregnation.

The performance test

The performance tests of both synthesized and commercial catalysts were conducted in a fixed bed quartz reactor (ID = 15 mm) and under atmospheric pressure, using a

mixture of propane and hydrogen (for dilution of propane in a gas mixture to increase propane conversion) with operation condition: (H_2/CH = 0.85; WHSV = 2 h^{-1} and T = 620 °C). The product was analyzed for light-hydrocarbons by an online gas chromatograph (Agilent 6890N) equipped with TCD and FID detectors.

Results and discussion

Characterization of the catalysts

TPR results

The effects of different contents of Ce, Zn and Co as the promoters on the reduction properties of catalysts were studied by TPR. The PD-IND catalyst showed three reduction peaks at 293, 695, and 843 °C [26]; the first peak was related to the reduction of Pt species. The second peak was related to the reduction of the Sn species, which interacted strongly with Pt, forming the PtSn alloy [3, 26]. The third peak was related to the reduction of tin oxides that interacted strongly with the support [26]. The profiles of H_2-TPR are shown in Figs. 1, 2, and 3. A comparison of the adsorption strength distribution was obtained by the deconvolution of the peaks using normal distribution functions. The TPR diagrams of the catalysts obtained by Ce are shown in Fig. 1. Pt–Sn–K–Ce/γ-Al_2O_3 catalysts showed two temperature reduction peaks. The first peak was related to the reduction of Pt oxides. As shown in Table 1, the ceria sample shifted the reduction peak of Pt oxides to the lower temperature, as compared with PD-IND. This revealed that Pt could interact preferably with CeO_2, rather than Al_2O_3 [3, 17, 18, 27, 28]. The Pt–Ce interactions

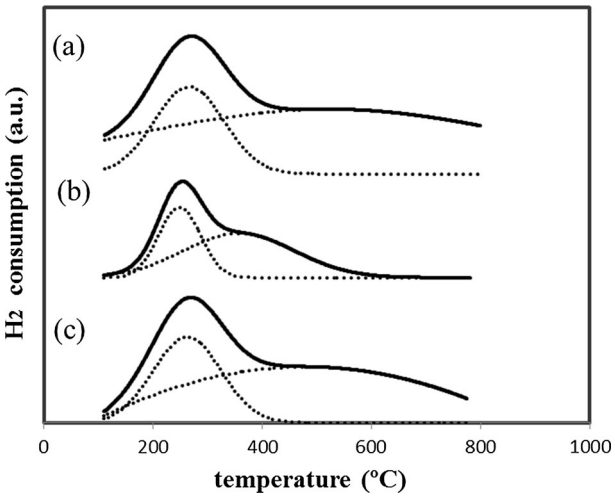

Fig. 1 H_2-TPR profiles of the samples with Ce as the promoter. **a** Pt–Sn–K–$Ce_{0.3}$/γ-Al_2O_3, **b** Pt–Sn–K–$Ce_{0.5}$/γ-Al_2O_3, **c** Pt–Sn–K–$Ce_{0.7}$/γ-Al_2O_3

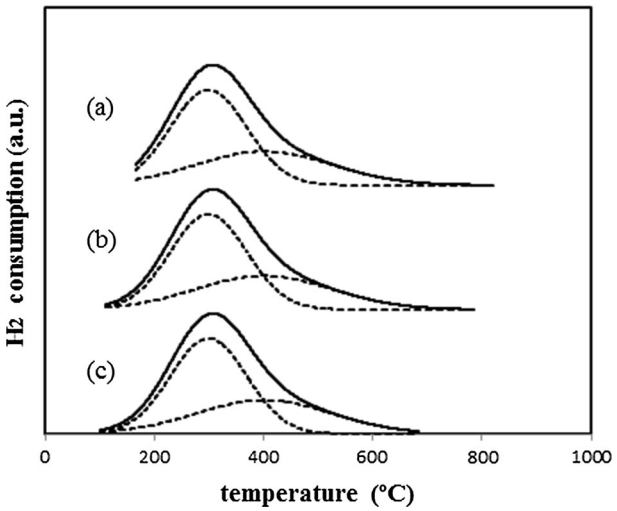

Fig. 2 H_2-TPR profiles of the samples with Zn as the promoter. **a** Pt–Sn–K–$Zn_{0.3}$/γ-Al_2O_3, **b** Pt–Sn–K–$Zn_{0.5}$/γ-Al_2O_3, **c** Pt–Sn–K–$Zn_{0.7}$/γ-Al_2O_3

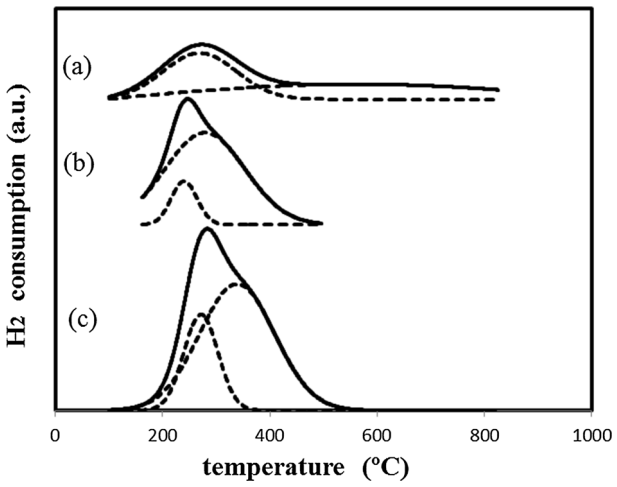

Fig. 3 H_2-TPR profiles of the samples with Co as the promoter. **a** Pt–Sn–K–$Co_{0.3}$/γ-Al_2O_3, **b** Pt–Sn–K–$Co_{0.5}$/γ-Al_2O_3, **c** Pt–Sn–K–$Co_{0.7}$/γ-Al_2O_3

could enhance the ability of Pt particles to resist agglomeration. Therefore, Pt–Sn–K–Ce/γ-Al_2O_3 could indicate high stability for propane dehydrogenation [3, 17, 27]. As can be seen in Table 1, the catalyst with 0.5 wt% of ceria showed the lowest Pt reduction peak temperature (248 °C) and slightly higher hydrogen consumption (0.15 mmol/g), as compared with Pt–Sn–K–$Ce_{0.3}$/γ-Al_2O_3 (0.1 mmol/g) and Pt–Sn–K–$Ce_{0.7}$/γ-Al_2O_3 (0.01 mmol/g). In contrast, the Pt–Sn–K–$Ce_{0.5}$/γ-Al_2O_3 catalyst showed the lowest Sn reduction temperature peak (359 < 520, 479 °C), and the corresponding peak areas were the least (0.23 mmol/g) too. In this way, judgment

Table 1 The results of TPR analysis

Catalyst	Low temperature peak		High temperature peak		Overall H_2 consumption mmol/g
	Reduction peak (°C)	H_2 consumption mmol/g	Reduction peak (°C)	H_2 consumption mmol/g	
Pt–Sn–K–$Ce_{0.3}$/γ-Al_2O_3	265	0.10	520	0.27	0.37
Pt–Sn–K–$Ce_{0.5}$/γ-Al_2O_3	248	0.15	359	0.23	0.38
Pt–Sn–K–$Ce_{0.7}$/γ-Al_2O_3	262	0.01	479	0.43	0.44
Pt–Sn–K–$Co_{0.3}$/γ-Al_2O_3	269	0.04	561	0.13	0.17
Pt–Sn–K–$Co_{0.5}$/γ-Al_2O_3	240	0.06	280	0.38	0.44
Pt–Sn–K–$Co_{0.7}$/γ-Al_2O_3	272	0.1	239	0.29	0.39
Pt–Sn–K–$Zn_{0.3}$/γ-Al_2O_3	301	0.37	401	0.23	0.6
Pt–Sn–K–$Zn_{0.5}$/γ-Al_2O_3	299	0.29	405	0.18	0.47
Pt–Sn–K–$Zn_{0.7}$/γ-Al_2O_3	299	0.11	401	0.06	0.17
Pt–Sn–K–$Ce_{0.5}$–$Zn_{0.7}$/γ-Al_2O_3	265	0.03	488	0.13	0.16
Pt–Sn–K–$Co_{0.3}$–$Zn_{0.7}$/γ-Al_2O_3	259	0.2	468	0.17	0.37

on the effect of ceria on the reduction of Sn would be difficult. This may be due to the metallic state of Sn. When Sn appears in a metallic state (Sn^0), it may be a poison, but when it appears in a nonmetallic state (Sn^{4+} or Sn^{2+}), it acts as a promoter [5]. Thus, it is better for Sn reduction peaks to appear in the higher temperatures with less hydrogen consumption. Due to the Ce effect on hydrogen consumption, it can be concluded that the interactions between Sn species and the support are strengthened, and the presence of Ce can inhibit the reduction of Sn species according to other papers [3, 27].

Fig. 2 shows that Zn could not reduce the Pt temperature reduction peak, as compared with PD-IND. As can be seen in Table 1, with increasing Zn loading, the decrease in the Pt reduction peak area was observed (0.11 mmol/g for Pt–Sn–K–$Zn_{0.7}$/γ-Al_2O_3 0.29, 0.37). So Pt–Sn–K–$Zn_{0.3}$/γ-Al_2O_3 showed the highest Pt reduction peak area (0.37 mmol/g). Consonni [29] investigated that in the case of the Pt/ZnO sample, even at low reduction temperatures (200 °C), ZnO could be reduced to metallic Zn, resulting in the formation of PtZn alloy. It could be concluded that some amounts of Zn species might be reduced to metallic Zn; thus the formation of the PtZn alloy would be inevitable [10]. Because of the much more amount of PtZn alloy in the Pt–Sn–K–$Zn_{0.7}$/γ-Al_2O_3 catalyst, Pt could not reduce the hydrogen consumption, which was the lowest. Another reason for the decrease in Pt ability for reduction could be that the extra amount of Zn might have blocked the platinum particles, not allowing Pt to be reduced. As it is difficult to assign the second peak to a certain species, this peak could appertain to the reduction of platinum, tin and zinc species [10]. By increasing the zinc concentration, the Sn species reduction peak areas were decreased. It indicates that the interactions between Sn species and the support could be strengthened. This means Zn could

stabilize the oxidation states of Sn species, thereby contributing to the catalytic performance.

It can be seen in Fig. 3 that Co could reduce the Pt temperature reduction peak, as compared with PD-IND. According to Table 1, it is too difficult to judge the effect of different concentrations of Co. But it could be seen that by increasing Co loading, the hydrogen consumption was increased. The second peak might be related to the reduction of Sn alloyed by Pt and Co. In the Pt–Sn–K–$Co_{0.3}$/γ-Al_2O_3 catalyst, the second peak appeared in the higher temperature (561 °C), and the corresponding reduction peak area was the least, in comparison to other Co concentrations (0.13 mmol/g < 0.29, 0.38). This implied that 0.3 wt% Co could stabilize the oxidation state of Sn.

Table 1 and Fig. 4 show that Pt–Sn–K–$Ce_{0.5}$–$Zn_{0.7}$/γ-Al_2O_3 had much less hydrogen consumption of the Pt reduction peak (0.03 mmol/g), as compared with Pt–Sn–K–$Ce_{0.5}$/γ-Al_2O_3 (0.15 mmol/g) and Pt–Sn–K–$Zn_{0.7}$/γ-Al_2O_3 (0.11 mmol/g) catalysts. Separate figures are given in the Supplementary Information that represent H_2-TPR profiles of Pt–Sn–K–$Ce_{0.5}$–$Zn_{0.7}$/γ-Al_2O_3 (Fig. S1) and Pt–Sn–K–$Co_{0.3}$–$Zn_{0.7}$/γ-Al_2O_3 (Fig. S2). It is possible that Pt, Zn and Ce could form potent interaction in the Pt–Sn–K–$Ce_{0.5}$–$Zn_{0.7}$/γ-Al_2O_3 catalyst, causing Pt not to be able to be reduced to the metallic phase. The second peak of Pt–Sn–K–$Ce_{0.5}$–$Zn_{0.7}$/γ-Al_2O_3 appeared at the higher temperature (488 °C), as compare with Pt–Sn–K–$Ce_{0.5}$/γ-Al_2O_3 (359 °C) and Pt–Sn–K–$Zn_{0.7}$/γ-Al_2O_3 (401 °C), thereby showing the interaction that between Pt, Sn, Ce and Zn shifted the location of the Sn reduction peak to the higher temperature. Also the TPR profile of Pt–Sn–K–$Co_{0.3}$–$Zn_{0.7}$/γ-Al_2O_3 is shown in Fig. 4. Table 1 shows the first peak of Pt–Sn–K–$Co_{0.3}$–$Zn_{0.7}$/γ-

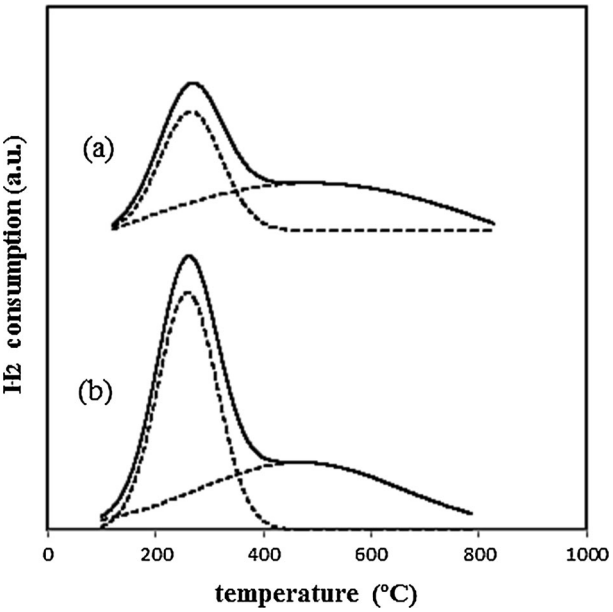

Fig. 4 H_2-TPR profile of **a** Pt–Sn–K–$Ce_{0.5}$–$Zn_{0.7}$/γ-Al_2O_3, **b** Pt–Sn–K–$Co_{0.3}$–$Zn_{0.7}$/γ-Al_2O_3

Al_2O_3, that was related to the reduction of Pt to metallic phase, was shifted to the lower temperature (259 °C), as compared to Pt–Sn–K–$Co_{0.3}$/γ-Al_2O_3 (269 °C) and Pt–Sn–K–$Zn_{0.7}$/γ-Al_2O_3 (299 °C). This revealed that the interaction between Pt, Zn and Co caused the easier reduction of Pt, and the corresponding reduction peak areas (0.2 mmol/g) were larger than Pt–Sn–K–$Co_{0.3}$/γ-Al_2O_3 (0.04 mmol/g) and Pt–Sn–K–$Zn_{0.7}$/γ-Al_2O_3 (0.11 mmol/g). However, H_2 consumption for the second peak of Pt–Sn–K–$Co_{0.3}$–$Zn_{0.7}$/γ-Al_2O_3 (0.17 mmol/g) was the highest, as compared with Pt–Sn–K–$Co_{0.3}$/γ-Al_2O_3 (0.13 mmol/g) and Pt–Sn–K–$Zn_{0.7}$/γ-Al_2O_3 (0.06 mmol/g). It means that the interaction between Sn, Zn and Co had no favorable effect on Sn reduction.

The results showed that all the samples, when compared with PD-IND, could eliminate the third peak which was related to the reduction of Sn^{+2} to Sn^0, acting as the poison and reducing the conversion and selectivity of the catalyst.

XRF results

Table 2 shows the results of the elemental analysis of the catalysts after calcination and reduction. It shows that the maximum Pt uptake occurred in the catalyst with the Zn promoter; especially, in Pt–Sn–K–$Zn_{0.5}$/γ-Al_2O_3 (0.47 wt%) and Pt–Sn–K–$Zn_{0.3}$/γ-Al_2O_3 (0.47 wt%), it was very close to the nominal value (0.5 wt%). It means that catalyst with Zn as the promoter could achieve a higher loading of active metal than Ce and Co did; this could be advantageous both from an economic viewpoint due to the high impregnation efficiency and the potentially higher catalyst conversion [30]. Pt–Sn–K–$Zn_{0.5}$/γ-Al_2O_3 and Pt–Sn–K–$Zn_{0.3}$/γ-Al_2O_3could uptake more Pt than Pt–Sn–K–$Zn_{0.7}$/γ-Al_2O_3 (0.43 wt%). By increasing the Zn concentration to 0.7 wt%, the extra amount of Zn could block the platinum particles or change the character of active metal by the formation of PtZn alloy that could improve the selectivity toward propylene, but the catalyst could loosen the conversion [10]. Due to this phenomenon, the adsorption of Pt was decreased. This was confirmed by TPR test. In this case, in Pt–Sn–K–$Zn_{0.5}$/γ-Al_2O_3 and Pt–Sn–K–

Table 2 The results of XRF analysis

Sample	Pt (wt%)	K_2O (wt%)	Cl (wt%)
Industrial catalyst (PD-IND)	0.36	0.98	1.20
Pt–Sn–K–$Zn_{0.3}$/γ-Al_2O_3	0.47	0.70	0.78
Pt–Sn–K–$Zn_{0.5}$/γ-Al_2O_3	0.47	0.68	0.70
Pt–Sn–K–$Zn_{0.7}$/γ-Al_2O_3	0.43	0.68	0.80
Pt–Sn–K–$Co_{0.3}$/γ-Al_2O_3	0.47	0.77	1.09
Pt–Sn–K–$Co_{0.5}$/γ-Al_2O_3	0.44	0.62	0.97
Pt–Sn–K–$Co_{0.7}$/γ-Al_2O_3	0.43	0.69	0.98
Pt–Sn–K–$Ce_{0.3}$/γ-Al_2O_3	0.33	0.62	0.93
Pt–Sn–K–$Ce_{0.5}$/γ-Al_2O_3	0.43	0.69	0.88
Pt–Sn–K–$Ce_{0.7}$/γ-Al_2O_3	0.38	0.68	0.74
Pt–Sn–K–$Co_{0.3}$–$Zn_{0.7}$/γ-Al_2O_3	0.45	0.63	0.79
Pt–Sn–K–$Ce_{0.5}$–$Zn_{0.7}$/γ-Al_2O_3	0.37	0.70	0.74

$Zn_{0.3}/\gamma$-Al_2O_3 catalysts, the amount of hydrogen consumption of the Pt reduction peak was higher than that of Pt–Sn–K–$Zn_{0.7}/\gamma$-Al_2O_3, showing that more Pt, rather than Pt–Sn–K–$Zn_{0.7}/\gamma$-Al_2O_3, could be reduced to metallic phases. It means that the more Pt uptake occurred on Pt–Sn–K–$Zn_{0.5}/\gamma$-Al_2O_3 and Pt–Sn–K–$Zn_{0.3}/\gamma$-Al_2O_3 catalysts. Among other contents of Ce, the Pt–Sn–K–$Ce_{0.5}/\gamma$-Al_2O_3 catalyst achieved higher Pt loading (0.43 wt%). Adequate amounts of Ce addition could prevent Pt agglomeration, so the Pt adsorption on Pt–Sn–K–$Ce_{0.5}/\gamma$-$Al_2O_3$was increased. By increasing the Ce amount loading, the extra Ce could block the Pt species, causing the reduction of the Pt uptake. The results obtained by TPR also showed that Pt–Sn–K–$Ce_{0.5}/\gamma$-Al_2O_3 catalyst had the lowest Pt reduction peak and the largest corresponding reduction peak area among other catalysts with the Ce promoter. It confirmed the results by XRF. On Pt–Sn–K–$Co_{0.3}/\gamma$-Al_2O_3 catalyst, there was more Pt uptake (0.47 wt%), as compared with Pt–Sn–K–$Co_{0.5}/\gamma$-Al_2O_3 (0.44 wt%) and Pt–Sn–K–$Co_{0.7}/\gamma$-Al_2O_3 (0.43 wt%). As can be seen in Table 2, by increasing the amount of Co loading, the Pt uptake was decreased. This means that Co could prevent the Pt adsorption. The much less amount of the Pt uptake in Pt–Sn–K–$Ce_{0.5}$–$Zn_{0.7}/\gamma$-Al_2O_3 (0.37 wt%), as compared with Pt–Sn–K–$Zn_{0.7}/\gamma$-Al_2O_3 (0.43 wt%) and Pt–Sn–K–$Ce_{0.5}/\gamma$-Al_2O_3 (0.43 wt%), showed that the synergic effect of the best concentration of Ce and Zn could not be suitable for Pt up taking. The presence of cobalt with 0.7 wt% of Zn improved the Pt uptake in Pt–Sn–K–$Co_{0.3}$–$Zn_{0.7}/\gamma$-Al_2O_3 (0.45 wt%), rather than Pt–Sn–K–$Zn_{0.7}/\gamma$-Al_2O_3 (0.43 wt%).

SEM results

In order to determine the uniformity of the particles of the Pt–Sn–K–$Co_{0.3}$–$Zn_{0.7}/\gamma$-Al_2O_3 catalyst deposited by impregnating on the spheres of γ-Al_2O_3, a characterization was done by scanning electronic microscope (SEM). Figure 5 shows two photographs of a calcined sample. This figure shows that the catalyst had uniform dispersion. It is believed that zinc serves as an efficient spacer to reduce the size of platinum ensembles, just as tin acts as a spacer in the Pt–Sn catalyst [31, 32, 34]. So this uniformity could be the result of the synergy effect of Sn and Zn in the Pt–Sn–K–$Co_{0.3}$–$Zn_{0.7}/\gamma$-Al_2O_3 catalyst. It was observed that the crystalline size was in the 4–10 μm range.

EDAX results of the Pt content on the edge and the center, and the middle of the edge and the center of them are shown in Table 3. Table 3 shows that Pt dispersion on three sides of this catalyst was nearly uniform, which could cause Sn and Zn to act as promoters.

TGA analysis

The TG-DTG profiles of the deactivated Pt–Sn–K–$Co_{0.3}$–$Zn_{0.7}/\gamma$-Al_2O_3 catalyst are plotted in Fig. 6. Two distinct peaks were identified from the DTG curve. The first region was around 100 °C, which was attributed to the removal of the adsorbed steam. The second peak ($400 \leq T \leq 550$ °C) was due to the combustion of coke deposited on the active metal and support sites; it is known as hard coke, which consists, for example, of poly nuclear aromatic compounds [33, 34]. The total lost

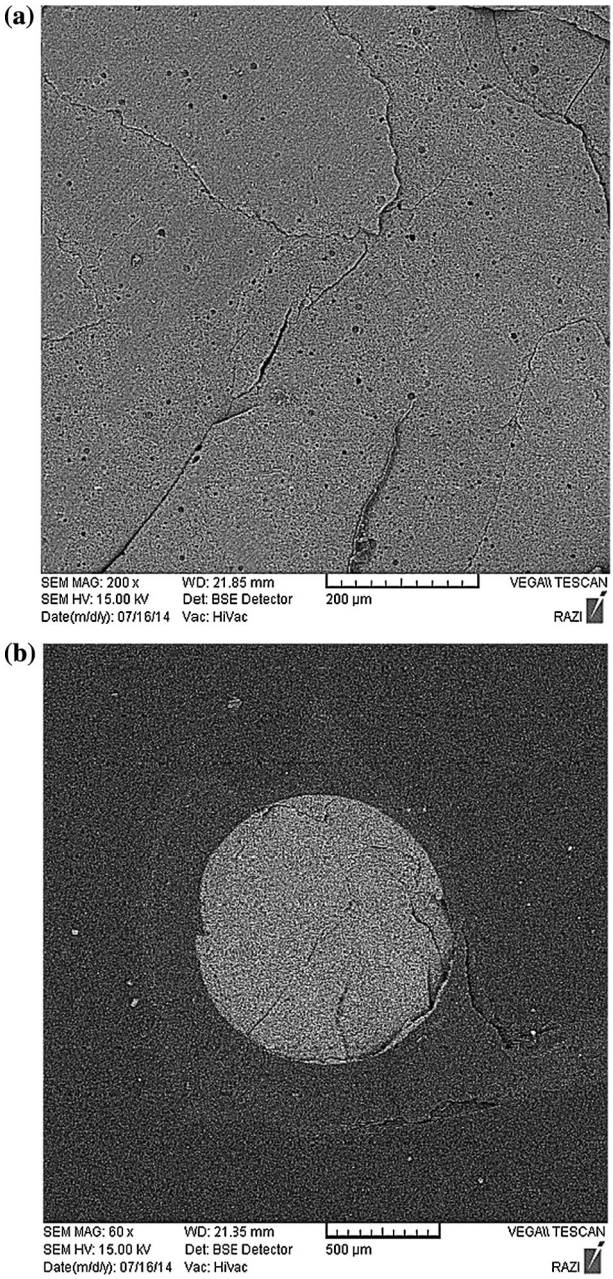

Fig. 5 SEM microphotographies of the Pt–Sn–K–$Co_{0.3}$–$Zn_{0.7}$/γ-Al_2O_3 catalyst. **a** top view and **b** sectional view

Table 3 The results of SEM analysis

Element	Center (wt%)	Edge (wt%)	Middle (wt%)
Pt	0.49	0.45	0.59

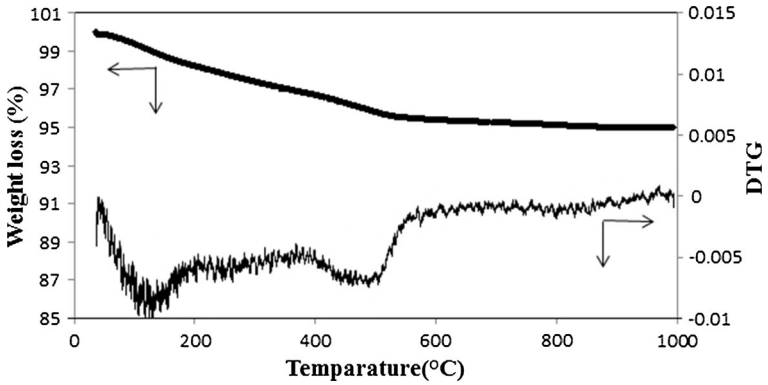

Fig. 6 TG-DTG profiles of the deactivated Pt–Sn–K–$Co_{0.3}$–$Zn_{0.7}$/γ-Al_2O_3 catalyst

weight was 4.994 (%w/w); 3.252 (%w/w) of this loss was related to water vapor and hydrocarbons, and only 1.741 (%w/w) belonged to coke combustion.

UV analysis

Table 4 shows the initial Pt concentration on the impregnation solvent before impregnation and the final Pt concentration after impregnation was obtained by the UV–Vis spectrometer. Pt–Sn–K–$Zn_{0.3}$/γ-Al_2O_3 (91.4%) and Pt–Sn–K–$Zn_{0.5}$/γ-Al_2O_3 (91.4%) adsorbed agreater percentage of platinum in the impregnation solution than Pt–Sn–K–$Zn_{0.7}$/γ-Al_2O_3 (90%) did, thereby confirming the results of XRF analysis. In the $Co(NO_3)_2$ and $Ce(NO_3)_3$ solutions, Pt adsorption was not largely affected by different amounts of Ce and Co, but they had a better effect on Pt adsorption than Zn in the impregnation solvent. In comparison with Pt–Sn–K–$Zn_{0.7}$/γ-Al_2O_3 (90%), the presence of Co and Ce with Zn (Pt–Sn–K–$Ce_{0.5}$–$Zn_{0.7}$/γ-Al_2O_3 and Pt–Sn–K–$Co_{0.3}$–$Zn_{0.7}$/γ-Al_2O_3) improved the percentage of Pt adsorption during Pt impregnation.

Performance results

The effects of Ce, Zn and Co promoters on the performance of the Pt–Sn–K/γ-Al_2O_3 catalyst in propane dehydrogenation are shown in Figs. 7, 8 and 9. It could be seen that all catalysts showed conversion decay during time-on-stream, thereby indicating that the catalyst deactivation was probably due to coke deposits. Fig. 7 shows that all the catalysts with Ce could increase conversion, as compared with PD-IND. These results indicated that Ce, by acting as the promoter, could promote the catalytic performance for propane dehydrogenation. However, the addition of

Table 4 The results of UV-analysis

Run no.	Solution specification	Initial Pt concentration (mmol/l)	Final Pt concentration (mmol/l)	Percent of adsorption (%)
1	Pt–Sn–K–$Zn_{0.3}$/γ-Al_2O_3	7.0	0.6	91.4
2	Pt–Sn–K–$Zn_{0.5}$/γ-Al_2O_3	7.0	0.6	91.4
3	Pt–Sn–K–$Zn_{0.7}$/γ-Al_2O_3	7.0	0.7	90
4	Pt–Sn–K–$Co_{0.3}$/γ-Al_2O_3	7.0	0.5	93
5	Pt–Sn–K–$Co_{0.5}$/γ-Al_2O_3	7.0	0.5	93
6	Pt–Sn–K–$Co_{0.7}$/γ-Al_2O_3	7.0	0.5	93
7	Pt–Sn–K–$Ce_{0.3}$/γ-Al_2O_3	7.0	0.5	93
8	Pt–Sn–K–$Ce_{0.5}$/γ-Al_2O_3	7.0	0.5	93
9	Pt–Sn–K–$Ce_{0.7}$/γ-Al_2O_3	7.0	0.5	93
10	Pt–Sn–K–$Ce_{0.5}$–$Zn_{0.7}$/γ-Al_2O_3	7.0	0.5	93
11	Pt–Sn–K–$Co_{0.3}$–$Zn_{0.7}$/γ-Al_2O_3	7.0	0.6	91.4

0.5 and 0.7 (wt%) of Ce resulted in a small increase in propylene selectivity, as compared with PD-IND (Fig. 7). For more clarity of propane conversion and propylene selectivity data for catalysts with Ce, these graphs are given in separate figures in the Supplementary Information, Figs. S3 and S4. It could be due to the lower Pt reduction peak temperature of the catalyst with Ce as a promoter, rather than PD-IND catalyst in TPR analysis. Pt–Sn–K–$Ce_{0.3}$/γ-Al_2O_3 had the highest conversion (initial: 48%, final: 40%); However, the propylene selectivity was poorest in Pt–Sn–K–$Ce_{0.3}$/γ-Al_2O_3. It could be the result of the significant rates of hydrogenolysis and coke reactions. As can be seen, when the cerium loading was increased, the enhancement in conversion was observed. However, when the cerium loading was 0.5 wt%, the propane selectivity was improved; while the higher cerium concentration (0.7 wt%) caused a decrease in the selectivity. These changes in propane selectivity by increasing the Ce loading could be because, when the loading of Ce was partly low, the surface of the support was not changed properly and covered with a low amount of Ce [18]. Suitable amounts of Ce addition could prevent Pt agglomeration, thus increasing metal dispersion [27]. However, when the excess loading of Ce resulted in a strong interaction between Ce and the support, it altered the support nature and the excessive Ce could block the Pt particles and further weaken the catalyst performance [3, 18, 27]. The best performance of the catalyst based on the suitable amount of Ce (Pt–Sn–K–$Ce_{0.5}$/γ-Al_2O_3); it could be defined as the catalyst achieving higher Pt loading, as compared to other amounts of Ce, based on XRF analysis. Also, the TPR results proved that catalyst with an appropriate amount of cerium, could reduce the Pt reduction peak temperature and increase hydrogen consumption.

It has been reported that the main role of CeO_2 is promoting the thermal stability of γ-Al_2O_3 against surface area loss in high temperature dehydrogenation conditions by preventing the transformation of γ-Al_2O_3 to α-Al_2O_3 [3, 17]. This effect of Ce is

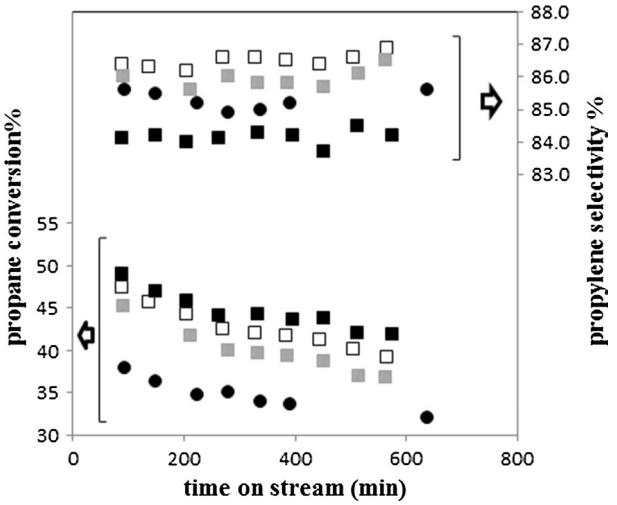

Fig. 7 Propane conversion and propylene selectivity of Pt–Sn-K-$Ce_{0.3}$ (filled square), Pt–Sn–K–$Ce_{0.5}$ (open square), Pt–Sn–K–$Ce_{0.7}$ (filled square), and PD-IND (filled circle) on γ- alumina supports (WHSV = 2 h^{-1}; T = 620 °C; H_2/CH = 0.85)

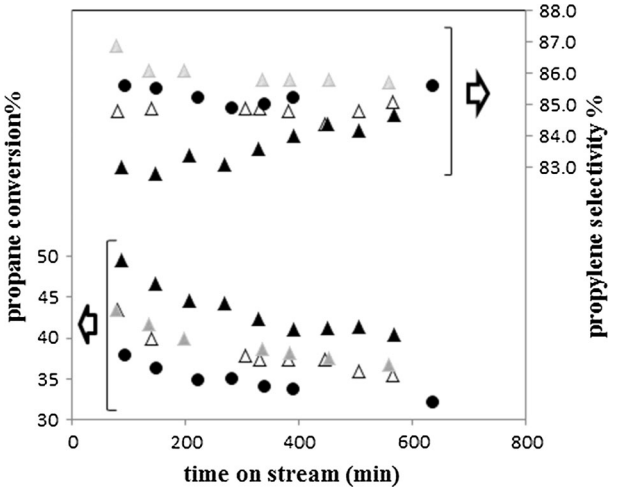

Fig. 8 Propane conversion and propylene selectivity of Pt–Sn–K–$Zn_{0.3}$ (filled triangle), Pt–Sn–K–$Zn_{0.5}$ (open triangle), Pt–Sn–K–$Zn_{0.7}$ (filled triangle), and PD-IND (open circle) on γ-alumina supports (WHSV = 2 h^{-1}; T = 620 °C; H_2/CH = 0.85)

related to the formation of Ce^{3+} as $CeAlO_3$ under the reducing atmosphere; it involves occupying vacant octahedral sites on the alumina surface, thereby blocking the transition of Al^{3+} cations from tetrahedral to octahedral sites during high-temperature treatment; however this phenomenon results in the loss of the surface area of alumina [1, 18–20]. This modification can not only improve the catalytic conversion, but also decline the amount of coke formation. So the selectivity can be

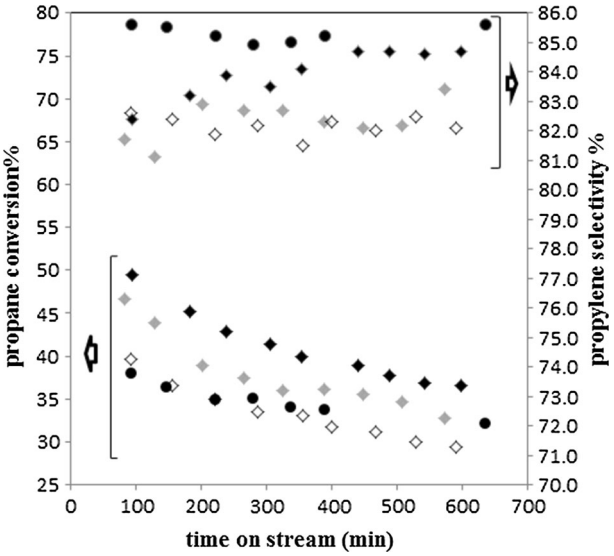

Fig. 9 Propane conversion and propylene selectivity of Pt–Sn–K–$Co_{0.3}$ (filled diamond), Pt–Sn–K–$Co_{0.5}$ (open diamond), Pt–Sn–K–$Co_{0.7}$ (filled diamond), and PD-IND (filled circle) on γ-alumina supports (WHSV = 2 h^{-1}; T = 620 °C; H_2/CH = 0.85)

significantly increased. The high oxygen storage capacity of ceria could result in oxygen vacancies at the metal–oxide interface of reduced ceria [35]. This oxygen storage capacity of ceria develops the cerium cations ability to cycle between + 4 and + 3 oxidation states under reducing conditions [19], which could decrease the coke formation on the catalyst surface. Because of all these reasons, catalysts developed by Ce as the promoter show good selectivity in propane dehydrogenation.

Propylene yield was calculated according to propylene selectivity and propane conversion. In Fig. S5 in the Supplementary Information, the results showed that the use of Ce as the promoter, as compared with PD-IND, could improve the propylene yield. So, the progress in the overall dehydrogenation performance was obtained by the addition of Ce to the Pt–Sn–K/γ-Al_2O_3 catalyst.

Fig. 8 shows that all contents of Zn could increase conversion more than PD-IND did. This suggested that zinc could promote the catalytic performance for propane dehydrogenation. The reason for this improvement could be the geometric and electronic modifications of the metallic phase that occurred when Zn was used as the promoter in the Pt–Sn–K/γ-Al_2O_3 catalyst. These modifications improved catalytic performance [13]. The geometric modifications included enhancement of Pt dispersion and the reduction of the platinum ensembles size [4, 10]. It is well known that propylene is produced on the single platinum atom as an active site, while hydrogenolysis and coke reactions need large platinum particles. So, the use of Zn in Pt-based catalysts can reduce the size of the platinum particles due to the role of tin in PtSn catalyst and decrease the hydrogenolysis and coke reactions which need large platinum ensembles; furthermore, Zn leads to increased conversion, and improved propylene selectivity and catalyst lifetime [4]. Zn, as

an electropositive, can change the electronic properties of Pt atoms (the formation of $Pt^{\delta-}$–$Zn^{\delta+}$ entities) [4, 10, 13]. The possibility of the formation of PtZn alloy has been reported in many papers [4, 10, 13, 31, 36–38]. This results in increasing the electronic density of the Pt surface by the addition of the electropositive metal (Zn) to platinum; this could weaken the strength of the Pt–(C=C) bond and facilitate the desorbtion of propylene as the coke precursor, as well suppressing the side reactions. All these could lead to enhancing the selectivity towards propylene [13]. As shown in Fig. 8, after loading with 0.3 wt% Zn, the catalyst showed the best conversion (initial: 49%, final: 40%). With increasing the zinc content to 0.5 and 0.7 wt%, the catalyst conversion was decreased, as compared with Pt–Sn–K–$Zn_{0.3}$/γ-Al_2O_3; it could because the extra amount of Zn blocked the platinum particles or reclaimed the character of the active metal. When the concentration of Zn is the excessive, the formation of PtZn alloy is inevitable. Therefore, because of the inactive nature of this alloy, metal dispersion was decreased, and the catalyst lost conversion. The alloyed Zn atoms, as well as the PtZn alloy phase, could increase the electronic density of the Pt metal. So, hydrogenolysis and coke reactions were suppressed; furthermore the selectivity toward propylene could be increased with the enhancement of Zn concentration [10]. The Pt–Sn–K–$Zn_{0.7}$/γ-Al_2O_3 catalyst, due to the formation of PtZn alloy, had the highest propylene selectivity (initial: 86.9%, final: 85.7%), as compared with Pt–Sn–K–$Zn_{0.5}$/γ-Al_2O_3 (initial: 84.8%, final: 85.1%) and Pt–Sn–K–$Zn_{0.5}$/γ-Al_2O_3 (initial: 83%, final: 84.7%). As TPR showed less hydorgen consumption of the second peak of Pt–Sn–K–$Zn_{0.7}$/γ-Al_2O_3 catalyst (0.6 mmol/g), as compared with Pt–Sn–K–$Zn_{0.5}$/γ-Al_2O_3 (0.18 mmol/g) and Pt–Sn–K–$Zn_{0.3}$/γ-Al_2O_3 (0.23 mmol/g), better Pt–Sn–K–$Zn_{0.7}$/γ-Al_2O_3 catalyst performance could be expected. In addition, Pt–Sn–K–$Zn_{0.7}$/γ-Al_2O_3 could increase the selectivity toward propylene, as compared with PD-IND. It should be noted that separate conversion and selectivity graphs for these catalysts are showen in the Supplementary Information (Fig. S6 and S7). The yield profiles (Fig. S8) in the Supplementary Information show the overall improvement in the catalytic performance of zinc-doped PtSn catalyst, as compared with PD-IND.

In Fig. 9, the highest dehydrogenation performance was obtained for a Pt–Sn–K–$Co_{0.3}$/γ-Al_2O_3 catalyst. This better conversion and selectivity of Pt–Sn–K–$Co_{0.3}$/γ-Al_2O_3could be due to the stabilization effect of 0.3 wt% of cobalt on the oxidation state of Sn, as obtained by TPR analysis. Conversion of Pt–Sn–K–$Co_{0.3}$/γ-Al_2O_3 (initial: 49.5%, final: 36.5%) and Pt–Sn–K–$Co_{0.7}$/γ-Al_2O_3 (initial: 46.7%, final: 32.7%) catalysts was higher, as compared with PD-IND (initial: 37.9%, final: 32.1%), The figure for propane conversion (Fig. S9) is given in the Supplementary Information; however, PD-IND obtained the highest selectivity among the catalysts. Pt–Sn–K–$Co_{0.3}$/γ-Al_2O_3 showed better conversion and selectivity, as compared with other catalysts, by Co. The more clear figures for propylene selectivity (Fig. S10) and yield profile (Fig. S11) are shown in the Supplementary Information. Also, the XRF test showed that on the Pt–Sn–K–$Co_{0.3}$/γ-Al_2O_3 catalyst, there was more Pt uptake, as compared with other contents of Co. In addition, XRF showed Co could prevent the Pt adsorption; this might be one possible reason for the poorest performance, as compared with catalysts using Zn and Ce as the promoter. Pt–Sn–K–$Ce_{0.5}$/γ-Al_2O_3, Pt–Sn–K–$Co_{0.3}$/γ-Al_2O_3 and Pt–Sn–K–$Zn_{0.7}$/γ-Al_2O_3 catalysts

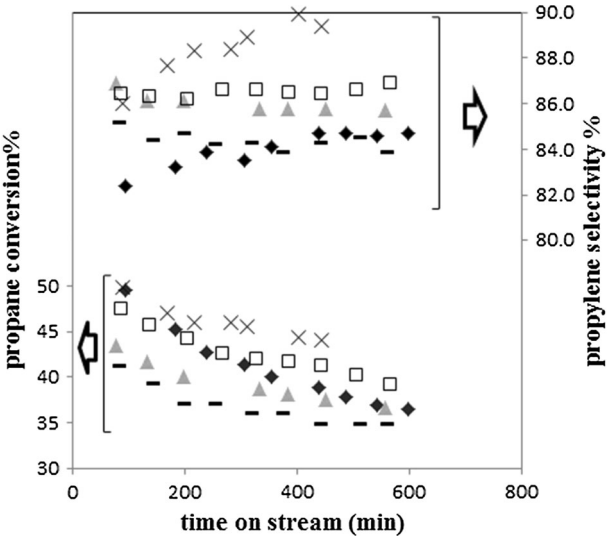

Fig. 10 Propane conversion and propylene selectivity of Pt–Sn–K–$Co_{0.3}$ (filled diamond), Pt–Sn–K–$Ce_{0.5}$ (open square), Pt–Sn–K–$Zn_{0.7}$ (filled triangle), Pt–Sn–K–$Ce_{0.5}$–$Zn_{0.7}$ (dashed line), and Pt–Sn–K–$Co_{0.3}$–$Zn_{0.7}$ (times) on γ-alumina supports (WHSV = 2 h^{-1}; T = 620 °C; H_2/CH = 0.85)

were chosen as the best catalysts among other concentrations of Ce, Co and Zn because of their higher selectivity. Therefore, Pt–Sn–K–$Ce_{0.5}$–$Zn_{0.7}$/γ-Al_2O_3 and Pt–Sn–K–$Co_{0.3}$–$Zn_{0.7}$/γ-Al_2O_3 catalysts were prepared. Their performances are shown in Fig. 10. (These results for conversion, selectivity and yield, in detail, are given in Fig. S12, S13 and S14 in the Supplementary Information). The highest dehydrogenation conversion, selectivity and yield among all the catalysts, were obtained for Pt–Sn–K–$Co_{0.3}$–$Zn_{0.7}$/γ-Al_2O_3 (conversion: initial: 50%, final: 44%, selectivity: initial: 86% final: 90%). The synergic effect between Co and Zn could enlarge the Pt reduction peak areas more than Pt–Sn–K–$Co_{0.3}$/γ-Al_2O_3 and Pt–Sn–K–$Zn_{0.7}$/γ-Al_2O_3; so it could improve the catalyst performance. The presence of cobalt and zinc as the electropositive element could improve the Pt electronic density and suppress the coke formation; therefore, it could improve conversion and selectivity. The addition of Ce (0.5%) to Pt–Sn–K/γ-Al_2O_3 catalyst resulted in a better performance, as compared with Co and Zn addition; also, Pt–Sn–K–$Zn_{0.7}$/γ-Al_2O_3 showed better selectivity and less conversion in comparison to Pt–Sn–K–$Co_{0.3}$/γ-Al_2O_3. As shown in Fig. 10, Pt–Sn–K–$Ce_{0.5}$–$Zn_{0.7}$/γ-Al_2O_3 catalyst had the poorest selectivity. The less hydrogen consumption of the Pt reduction peak, rather than Pt–Sn–K–$Ce_{0.5}$/γ-Al_2O_3 and Pt–Sn–K–$Zn_{0.7}$/γ-Al_2O_3, could be responsible for the weak performance of Pt–Sn–K–$Ce_{0.5}$–$Zn_{0.7}$/γ-Al_2O_3, as compared with other catalysts (Fig. S14 in the Supplementary Information). Also, XRF results conceded that Pt–Sn–K–$Ce_{0.5}$–$Zn_{0.7}$/γ-Al_2O_3 could get a less amount of Pt than Pt–Sn–K–$Zn_{0.7}$/γ-Al_2O_3 and Pt–Sn–K–$Ce_{0.5}$/γ-Al_2O_3 did, so performance was dropped.

Stability test of the Pt–Sn–K–$Co_{0.3}$–$Zn_{0.7}$/γ-Al_2O_3 catalyst

A stability test of the Pt–Sn–K–$Co_{0.3}$–$Zn_{0.7}$/γ-Al_2O_3 catalyst was also carried out. The propane conversion and the selectivity to propylene as the major products, and selectivity of by-products including methane, ethane and ethylene are shown in Fig. S15 in the Supplementary Information, as a function of the reaction time. It can be seen that conversion was dropped continuously with time on stream; the main reason of this deactivation was carbon deposition. For the first hours of reaction, selectivity of propylene was increased, as these deposits acted as inactive species which inhibited the undesired reactions [27]. The selectivity of propylene started to drop out after around 33 h, since the amount of the carbon deposition was increased, thereby blocking the active site of the reaction, which was accompanied by the increase in by-product selectivity.

Conclusions

Ce exhibited superior promoting effects on the Pt–Sn–K/γ-Al_2O_3 catalyst in the dehydrogenation of propane as shown by the general comparison of Zn, Ce and Co as the promoter. This effect could be attributed to promoting the thermal stability of γ-Al_2O_3. The Pt–Ce interactions could enhance the ability of Pt particles to resist agglomeration, as specified by TPR analysis. These effects could increase selectivity significantly. Among the catalyst samples synthesized by different amounts of Ce, Zn and Co loading, Pt–Sn–K–$Ce_{0.5}$/γ-Al_2O_3, Pt–Sn–K–$Zn_{0.7}$/γ-Al_2O_3 and Pt–Sn–K–$Co_{0.3}$/γ-Al_2O_3 exhibited the highest propane dehydrogenation performance. Moreover, the Pt–Sn–K–$Co_{0.3}$-$Zn_{0.7}$/γ-Al_2O_3 showed the highest conversion and selectivity. The XRF measurements showed that Zn, probably due to the formation of PtZn alloy, could increase the Pt uptake. SEM analysis also revealed that that Zn could act as a spacer for the Pt particles. TGA analysis showed that this effect of Zn with the synergy effect of Co could reduce the amount of coke formation.

Acknowledgements The authors would like to thank Petrochemical Research and Technology Company (NPC-RT) for the financial support of this work.

References

1. Pisduangdaw S, Panpranot J, Chaisuk C, Faungnawakij K, Mekasuwandumrong O (2011) Catal Commun 330:1161–1165
2. Zhang Y, Zhou Y, Shi J, Zhou S, Zhang Z, Zhang S, Guo M (2013) Fuel Process Technol 36:94–104
3. Yu C, Ge Q, Xu H, Li W (2006) Appl Catal A 315:58–67
4. Wang Y, Wang Y, Wang S, Guo X, Zhang SM, Huang WP, Wu S (2009) Catal Lett 132:472–479
5. Zhang Y, Zhou Y, Wan L, Xue M, Duan Y, Liu X (2011) J Nat Gas Chem 20:639–646
6. Zhang Y, Zhou Y, Wan L, Xue M, Duan Y, Liu X (2011) Fuel Process Technol 92:1632–1638
7. Tasbihi M, Feyzi F, Amlashi MA, Abdullah AZ, Mohamed AR (2007) Fuel Process Technol 88:883–889
8. He SB, Bi WJ, Lai YL, Rong X, Yang X, Sun CL (2010) J Fuel Chem Technol 38:452–457
9. Lee MH, Nagaraja BM, Lee KW, Jung KD (2014) Catal Today 232:53–62

10. Zhang Y, Zhou Y, Shi J, Sheng X, Duan Y, Zhou S, Zhang Z (2012) Fuel Process Technol 96:220–227
11. Siri GJ, Bertolini GR, Casella ML, Ferretti OA (2005) Mater Lett 59:2319–2324
12. Armendariz H, Guzman A, Toledo JA, Llano ME, Vazquez A, Aguilar-Rios G (2001) Appl Catal A 211:69–80
13. Yu C, Xu H, Ge Q, Li W (2007) J Mol Catal A 266:80–87
14. Nagaraja BM, Jung H, Yang DR, Jung KD (2014) Catal Today 232:40–52
15. Del Angel G, Bonilla A, Pena Y, Navarrete J, Fierro JLG, Acosta DR (2003) J Catal 219:63–73
16. Navarro RM, Guil-Lopez R, Ismail AA, Al-Sayari SA, Fierro JLG (2015) Catal Today 242:60–70
17. Yu C, Ge Q, Xu H, Li W (2006) Catal Lett 112:197–201
18. Ma Z, Wang J, Li J, Wang N, An C, Sun L (2014) Fuel Process Technol 128:283–288
19. Damyanova S, Perez CA, Schmal M, Bueno JMC (2002) Appl Catal A 234:271–282
20. Costa-Nunes O, Ferrizz RM, Gorte RJ, Vohs JM (2005) Surf Sci 592:8–17
21. Guczi L, Bazin D, Kovacsa I, Borko L, Schaya Z, Lynch J, Parent P, Lafon C, Stefler G, Koppany ZS, Sajo I (2002) Top Catal 20:1–4
22. Dietrich PJ, Sollberger FG, Akatay MC, Stach EA, Delgass WN, Miller JT, Ribeiro FH (2014) Appl Catal B 156–157:236–248
23. Biloen P, Dautzenberg F, Sachtler W (1977) J Catal 50:77–86
24. Sattler JJHB, Ruiz-Martinez J, Santillan-Jimenez E, Weckhuysen BM (2014) Chem Rev 114:10613–10653
25. Sahebdelfar S, Tahriri Zangeneh F (2010) Iran J Chem Eng 7:51–58
26. Tahriri Zangeneh F, Sahebdelfar S (2011) Iran J Chem Eng 8:48–54
27. Xue M, Zhou Y, Zhang Y, Liu X, Duan Y, Sheng X (2012) J Nat Gas Chem 21:324–331
28. Vu BK, Song MB, Ahn IY, Suh YW, Suh DJ, Kim WI, Koh HL, Choi YG, Shin EW (2011) Catal Today 164:214–220
29. Consonni M, Jokic D, Yu Murzin D, Touroude R (1999) J Catal 188:165–175
30. Tahriri Zangeneh F, Mehrazma S, Sahebdelfar S (2013) Fuel Process Technol 109:118–123
31. Seo H, Lee JK, Hong UG, Park G, Yoo Y, Lee J, Chang H, Song IK (2014) Catal Commun 47:22–27
32. Zhang YW, Zhou YM, Qiu AD, Wang Y, Xu Y, Wu PC (2006) Catal Commun 129:860–866
33. Luo S, He S, Li X, Li J, Bi W, Sun C (2015) Fuel Process Technol 214:156–161
34. Simon E, Rosas JM, Santos A, Romero A (2013) Chem Eng J 214:119–128
35. Wang SB, Lu GQ (1998) Appl Catal B 19:267–277
36. Silvestre-Albero J, Serrano-Ruiz JC, Sepulveda-Escribano A, Rodrıguez-Reinoso F (2005) Appl Catal A 292:244–251
37. Bocanegra S, Ballarini A, Zgolicz P, Scelza O, de Miguel S (2009) Catal Today 143:334–340
38. Bocanegraa SA, Guerrero-Ruizb A, De Miguela SR, Scelza OA (2004) Appl Catal A 277:11–22